ChemComm

Halogenated UiO-66 Frameworks Display Superior Ability for Chemical Warfare Agent Simulant Degradation

Journal:	*ChemComm*
Manuscript ID	CC-COM-01-2019-000642.R1
Article Type:	Communication

ChemComm

COMMUNICATION

Halogenated UiO-66 Frameworks Display Superior Ability for Chemical Warfare Agent Simulant Degradation

Received 00th January 20xx,
Accepted 00th January 20xx

DOI: 10.1039/x0xx00000x

www.rsc.org/

Mark Kalaj, Mohammad R. Momeni, Kyle C. Bentz, Kyle S. Barcus, Joseph M. Palomba, Francesco Paesani, and Seth M. Cohen *

Herein, a series of halogenated UiO-66 derivatives was synthesized and analyzed for the breakdown of the CWA simulant dimethyl-4-nitrophenyl phosphate (DMNP) to analyze ligand effects. UiO-66-I degrades DMNP at a rate four times faster than the most active previously reported MOFs. MOF defects were quantified and ruled out as a cause for increased activity. Theoretical calculations suggest the enhanced activity of UiO-66-I originates from halogen bonding of the iodine atom to the phosphoester linkage allowing for more rapid hydrolysis of the P-O bond.

Despite broad condemnation across the globe and international agreements prohibiting their use, organophoshpate-based chemical warfare agents (CWAs) remain a danger. Indeed, it is an unfortunate and unsettling reality that these agents seem to be appearing more frequently in news cycles, even tied to events far from active war zones. There remains a pressing need to develop advanced materials to safeguard warfighters and civilians against CWAs.[1] Recently, some zirconium-based members of the class of porous, crystalline materials known as metal-organic frameworks (MOFs)[2] have demonstrated efficient catalytic degradation of these types of CWAs.[2c, 3] MOFs are constructed from inorganic metal nodes, termed secondary building units (SBUs) and multitopic organic linkers, forming highly porous three-dimensional lattices of varying complexity.[2, 4] The porosity of MOFs coupled with the catalytic activity from functional units on the ligands and/or active metal sites at the SBUs have made MOFs candidates for several applications.[5]

Whereas Zr-MOFs have been effective for CWA degradation of nerve agents and their simulants, the mechanism of hydrolysis remains relatively unknown from an experimental perspective. Most experimental work suggests catalysis is primarily due to the strong Lewis acidity of the metal center, although, more recently this catalytic activity has been specifically attributed to MOF defect sites.[3, 6] Density functional theory (DFT) calculations indicate the mechanism involves binding of nerve agent to the Zr^{4+} metal center followed by hydrolysis of the phosphoester bond resulting in agent degradation.[3b, 7] Two approaches have been used to enhance nerve agent hydrolysis in MOFs: synthesizing MOFs with different ligands or metal centers that improve hydrolysis, or by promoting defective sites at the SBU where catalytic conversion takes place.[6, 8] Because DFT calculations have suggested the importance of the SBU, most work in the literature has focused on engineering more catalytic sites into the SBU of the MOF.[7a, 8a] The only example of ligand derivatization improving CWA simulant degradation has been demonstrated by the addition of amine ($-NH_2$) functional groups on the MOF linkers.[6, 9] In the case of UiO-66, the amine functionalized derivative, UiO-66-NH_2, displays 20-fold higher activity than the parent MOF at pH = 10.[9] The significance of this amine functionality was also shown in a series of NU-1000 MOFs where *ortho* positioning of the amine groups displays 3-fold greater activity than the unfunctionalized canonical MOF.[6] The increased activity of these MOFs is thought to be a result of the amine working as a Brønsted base to synergistically enhance catalytic activity.[6, 7c, 9] Importantly, the catalytic activity of these MOFs is pH dependent.[10] Although UiO-66-NH_2 is a faster catalyst than UiO-66 at pH = 10, when examined at pH = 8, UiO-66 actually displays 2-fold faster activity than UiO-66-NH_2.[10]

Herein, the halogenated UiO-66 derivatives UiO-66-F, UiO-66-Cl, UiO-66-Br, and UiO-66-I (Figure 1) have been screened for the catalytic degradation of dimethyl-4-nitrophenyl phosphate (DMNP) using a high-throughput screening (HTS) method.[10] The UiO-66-I derivative displays ~4-fold greater catalytic activity than the parent UiO-66, while the other halogenated derivatives show no enhancement over unfunctionalized UiO-66. MOF defect sites were quantified via thermogravimetric analysis (TGA) indicating nearly identical defect sites across the

[a] *Department of Chemistry and Biochemistry, University of California, San Diego, La Jolla, CA, 92023-0358, USA. E-mail: scohen@ucsd.edu*
[b] *† Electronic Supplementary Information (ESI) available: Experimental procedures, 1HNMR, PXRD, TGA, and SEM. See DOI: 10.1039/x0xx00000x*

series. Computational analysis indicates that the more polarizable iodine moiety enables a halogen bonding effect that enhances the catalytic degradation of DMNP hydrolysis at the phosphoester linkage. To our knowledge, there are only two other reports in the literature where heterogenous catalysts have faster rates as a function of halogen bonding.[11] More specifically, in MOFs, previous reports of halogen bonding have been demonstrated as a means of crystal engineering,[12] but this is the first-time halogen bonding as a means of enhancing catalysis has been demonstrated in a MOF.

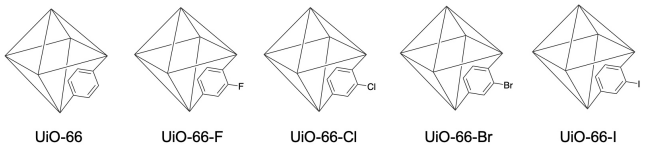

Figure 1. Chemical schematic of UiO-66 and the four halogenated UiO-66 MOFs used in this study.

The parent UiO-66 and all of the halogenated derivatives were synthesized using an acetic acid modulated synthesis.[5a] All MOF samples were digested in dilute acid and analyzed via ^{1}H NMR, confirming the ligands were intact after MOF synthesis (Figures S1-S9). Powder X-ray diffraction (PXRD) results confirm the formation of the MOF (Figure 2) and scanning electron microscopy (SEM) images show similar particle sizes (~200 nm) for all the samples (Figure S10-S15). All MOFs were also analyzed via N_2 gas sorption measurements to determine the surface area of the materials. The surface area of the MOFs decreased as the halogen size increases (F < Cl < Br < I) indicating the expected pore occupancy by the halogen (Figure 2).

The catalytic activity of these materials with the CWA simulant DMNP was evaluated using a previously validated HTS method.[10] DMNP is a safer alternative to CWAs, while most effectively mimicking the phosphoester linkage. Degradation of DMNP was monitored via UV-vis spectroscopy through the detection of the cleaved *p*-nitrophenol product (Figure 3). An equal mass (~6 mg) of MOF was utilized in each well for monitoring catalytic reactions. Rates were calculated to account for the substantial difference in moles of MOF catalyst between samples (due to the increased mass of the halogenated MOFs, see SI) so that a direct comparison could be made across all materials in this study. Reported rates are averages of seven replicates per sample across three independently prepared materials for each MOF. HTS evaluation of the five materials in Figure 1 at pH = 8 show that UiO-66-I is four times more active than the parent UiO-66 MOF and NU-1000 (vide infra). The UiO-66-I MOF displays the highest activity of any MOFs tested under these HTS assay conditions (96 total MOFs previously screened).[10] Previous studies have examined DMNP hydrolysis at predominantly two different pH conditions, pH = 8 and pH = 10;[10] experiments here were performed at pH = 8 to best emulate field conditions for potential contact with CWAs.

To further probe this ligand effect, we synthesized a mixed linker MOF (termed UiO-66-$I_{50\%}$) containing ~50% 1,4-benzenedicarboxylic acid (bdc^{2-}) linkers and ~50% I-bdc^{2-} that was characterized by PXRD and gas sorption measurements (Figure S16-S17). When screened for catalytic activity against DMNP, the mixed ligand UiO-66-$I_{50\%}$ performs better than UiO-66, but poorer than UiO-66-I indicating that increased iodine content in the MOF correlates with improved catalytic activity (Figure 3).

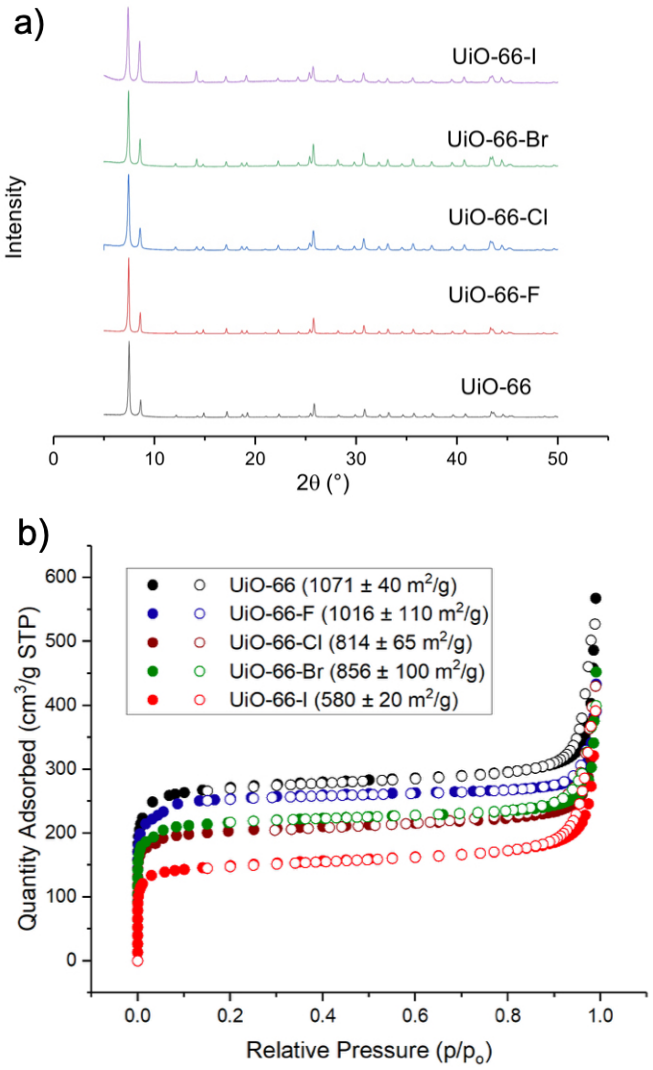

Figure 2. a) PXRD pattern of UiO-66 MOFs used in this study. b) N_2 sorption isotherms of UiO-66 MOFs: black traces are UiO-66, blue traces are UiO-66-F, brown traces are UiO-66-Cl, green traces are UiO-66-Br, and red traces are UiO-66-I.

TGA of the MOFs was conducted to quantify the missing ligand defects in the materials. Using the method developed by Lillerud et al. (see the Supporting Information for complete details) the defects in the UiO-66 materials were quantified. The results show similar levels of defects across all five of the MOFs used in this study (Figure 4).[13] Specifically, TGA data (Figure S18-S23) shows that each MOF contains about ten carboxylates per cluster, indicating ~2 missing carboxylate linkers per SBU (~17% ligand defect abundance, Figure 4). Therefore, the increased activity of UiO-66-I is not correlated with a difference in defects created during MOF synthesis using

the iodine functionalized linker. Furthermore, as expected, the BET surface area of the MOFs decreases with increasing size of the halogen indicating similar defect sites abundance across all of the MOF materials. Finally, the rate of DMNP degradation is not correlated with increasing halogen electronegativity (F > I) ruling out the possibility of the enhanced activity being due to an inductive electron withdrawing effect.

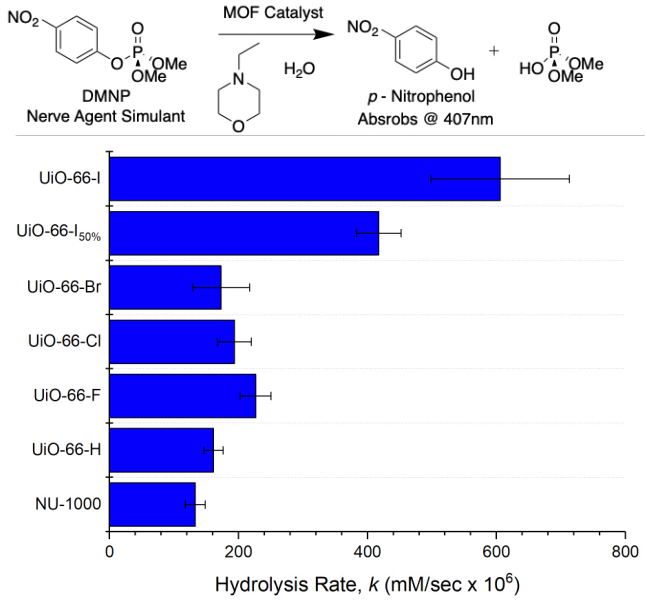

Figure 3. Top: DMNP degradation reaction. Bottom: Molar mass corrected rate of catalytic degradation of DMNP by MOFs measured by UV-visible absorption (407 nm) at pH = 8.

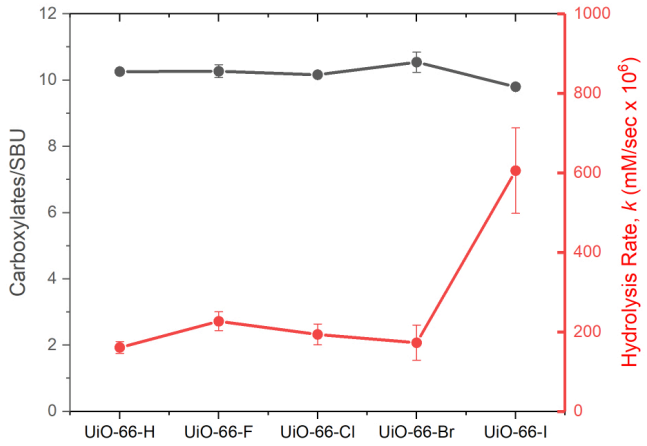

Figure 4. Ratio of organic linkers per SBU of UiO-66 MOFs (black) vs. rate of DMNP degradation by MOFs (red).

Halogen bonding is described as an interaction between an electrophilic region associated with a halogen atom and a nucleophilic region of another molecule.[14] The electrophilic region in the halogen atom is referred to as the sigma hole and this area increases as a function of halogen polarizability (e.g., I > Br > Cl > F).[14] Across the series of halogens, halogen bonding is rarely observed in the case of fluorine and chlorine, but more often with bromine and iodine.[14] Several examples in the halogen bonding literature dictate instances where, across a family of analogous materials, the halogen bond is only observed with the most polarizable iodine atom.[15]

To model the effect of halogen bonding on catalytic hydrolysis of DMNP, DFT M06-L[16] calculations were performed on different isolated SBU cluster models of UiO-66 and UiO-66-I. The models were built from the optimized periodic crystal structure of mono-defective UiO-66 (i.e., UiO-66 with one missing ligand) (see SI for details of the periodic and cluster calculations, Figures S26-S27). In the as-synthesized UiO-66-I, the relative position of the halogens on the bdc^{2-} linkers with respect to the zirconium SBU is random. Therefore, when examining an isolated cluster there arise three possible arrangements of the iodine atoms around the SBU. UiO-66-I cluster models were designed to model these three possible conformations: one with iodine groups in all *ortho (ortho*-UiO-66-I*)*, a second with all *meta* (*meta*-UiO-66-I), and a third, alternating *ortho*/*meta* substitution pattern (*alter*-UiO-66-I, Figure S27) with respect to the SBU. The aim of these calculations is not to quantitatively reproduce the experimental data, but rather to qualitatively describe the observed trends in catalytic activity and provide mechanistic insights. Recent mechanistic studies on DMNP hydrolysis on different MOFs have shown the nucleophilic attack by water on the phosphorous center to be the rate-limiting step and hence this was the focus of the calculations performed here on UiO-66 and UiO-66-I.[6, 17]

Theory shows that in both the *ortho*- and *alter*-UiO-66-I MOFs, the iodine atoms of the MOF and the methoxy groups of DMNP are involved in a strong halogen bond. The M06-L computed I–OMe bond distances in DMNP bonded and transition state structures of the *ortho*-UiO-66-I are 0.095 Å and 0.233 Å shorter than the sum of the van der Waals radii of the iodine and the oxygen atoms, respectively (Figure 5, Table S2). The computed activation free energies ($\Delta G^{\ddagger}$) for UiO-66, *ortho*-UiO-66-I, *meta*-UiO-66-I, and *alter*-UiO-66-I are 19.9, 11.0, 19.5, and 12.2 kcal/mol, respectively. Computed CM5 charges further confirm formation of the halogen bonding between iodine and -OMe group of the DMNP in both *ortho*- and *alter*-UiO-66-I systems (Table S1). This is in stark contrast to the *meta*-UiO-66-I MOF where the iodine atoms are positioned far away from the oxygen atoms of the DMNP bonded UiO-66 (>5.7 Å) resulting in similar $\Delta G^{\ddagger}$ values for water addition in *meta*-UiO-66-I and the parent UiO-66 (19.5 kcal/mol and 19.9 kcal/mol, respectively, Table S1). Overall, our calculations show that the sigma hole of the iodine atom forms a rather strong halogen bonding with the nucleophilic methoxy group of DMNP which in turn results in a more electrophilic oxygen atom on the DMNP molecule allowing hydrolysis to occur more readily. In conclusion, the halogenated UiO-66-I shows a substantially enhanced degradation of the CWA simulant DMNP. Theoretical calculations suggest that halogen bonding is the origin of this increased activity and facilitates the catalytic hydrolysis of the phosphoester linkage. These findings offer new avenues for designing MOFs to more rapidly degrade CWAs.

This work was supported by a grant from the Army Research Office, Department of Army Material command, under Award No. W911NF-16-2-0106 and from the National Science

Foundation under award CHE-1704063 for the theoretical calculations that were carried out on resources of the Extreme Science and Engineering Discovery Environment (XSEDE), which is supported by the National Science Foundation through grant ACI-1053575. This work was performed in part at the San Diego Nanotechnology Infrastructure (SDNI) of U.C. San Diego, a member of the National Nanotechnology Coordinated Infrastructure, which is supported by the National Science Foundation (Grant ECCS-1542148). M.K. is supported by the Department of Defense (DoD) through the National Defense Science and Engineering Graduate (NDSEG) Fellowship Program. M.K. would like to thank Korey P. Carter (Lawrence Berkeley National Lab) for helpful discussions.

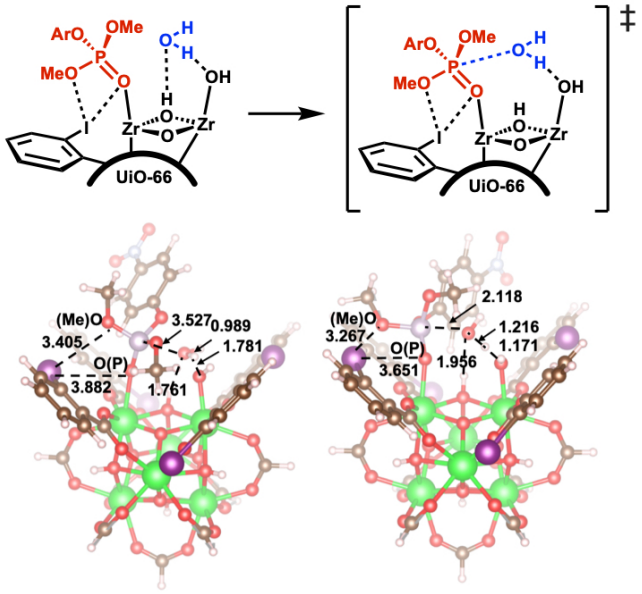

Figure 5. M06-L computed bond lengths (Å) in *ortho*-UiO-66-I cluster models of DMNP bonded (*left*) and transition state for nucleophilic attack of water to the P center (*right*) (ArO = 4-nitrophenoxide). Gray, white, red, blue, light purple, dark purple and green represent C, H, O, N, P, I, and Zr atoms, respectively.

Conflict of Interest

There are no conflicts to declare.

AUTHOR INFORMATION

Corresponding Author

scohen@ucsd.edu

Notes and references

[1] a) A. Hakonen, P. O. Andersson, M. Stenbæk Schmidt, T. Rindzevicius, M. Käll, *Anal. Chim. Acta.* **2015**, *893*, 1-13; b) A. Hakonen, T. Rindzevicius, M. S. Schmidt, P. O. Andersson, L. Juhlin, M. Svedendahl, A. Boisen, M. Käll, *Nanoscale* **2016**, *8*, 1305-1308.

[2] a) H. Furukawa, K. E. Cordova, M. O'Keeffe, O. M. Yaghi, *Science* **2013**, *341*, 1230444; b) O. M. Yaghi, M. O'Keeffe, N. W. Ockwig, H. K. Chae, M. Eddaoudi, J. Kim, *Nature* **2003**, *423*, 705-714; c) H. Li, M. Eddaoudi, M. O'Keeffe, M. Yaghi, *Nature* **1999**, *402*, 276-279.

[3] a) N. S. Bobbitt, M. L. Mendonca, A. J. Howarth, T. Islamoglu, J. T. Hupp, O. K. Farha, R. Q. Snurr, *Chem. Soc. Rev.* **2017**, *46*, 3357-3385; b) J. E. Mondloch, M. J. Katz, W. Bury, J. T. Hupp, W. C. Isley, 3rd, C. J. Cramer, P. Ghosh, P. Liao, R. Q. Snurr, G. W. Wagner, M. G. Hall, G. W. Peterson, J. B. DeCoste, O. K. Farha, *Nat. Mater.* **2015**, *14*, 512-516.

[4] a) M. Eddaoudi, J. Kim, N. Rosi, D. Vodak, J. Wachter, M. O'Keeffe, O. M. Yaghi, *Science* **2002**, *295*, 469-472; b) K. C. Bentz, S. M. Cohen, *Angew. Chem., Int. Ed.* **2018**, *57*, 14992-15001.

[5] a) M. S. Denny, Jr., S. M. Cohen, *Angew. Chem., Int. Ed.* **2015**, *54*, 9029-9032; b) M. S. Denny, M. Kalaj, K. C. Bentz, S. M. Cohen, *Chem. Sci.* **2018**, *9*, 8842-8849; c) M. Kalaj, M. Denny, K. Bentz, J. Palomba, S. M. Cohen, *Angew. Chem., Int. Ed.* **2018**.

[6] T. Islamoglu, M. A. Ortuno, E. Proussaloglou, A. J. Howarth, N. A. Vermeulen, A. Atilgan, A. M. Asiri, C. J. Cramer, O. K. Farha, *Angew. Chem., Int. Ed.* **2018**, *57*, 1949-1953.

[7] a) E. Lopez-Maya, C. Montoro, L. M. Rodriguez-Albelo, S. D. Aznar Cervantes, A. A. Lozano-Perez, J. L. Cenis, E. Barea, J. A. R. Navarro, *Angew. Chem., Int. Ed.* **2015**, *54*, 6790-6794; b) M. R. Momeni, C. J. Cramer, *Chem. Mater.* **2018**, *30*, 4432-4439; c) M. R. Momeni, C. J. Cramer, *ACS Appl. Mater. Interfaces* **2018**, *10*, 18435-18439.

[8] a) G. W. Peterson, M. R. Destefano, S. J. Garibay, A. Ploskonka, M. McEntee, M. Hall, C. J. Karwacki, J. T. Hupp, O. K. Farha, *Chem. Eur. J.* **2017**, *23*, 15913-15916; b) T. Islamoglu, A. Atilgan, S.-Y. Moon, G. W. Peterson, J. B. DeCoste, M. Hall, J. T. Hupp, O. K. Farha, *Chem. Mater.* **2017**, *29*, 2672-2675.

[9] M. J. Katz, S.-Y. Moon, J. E. Mondloch, M. H. Beyzavi, C. J. Stephenson, J. T. Hupp, O. K. Farha, *Chem. Sci.* **2015**, *6*, 2286-2291.

[10] J. M. Palomba, C. V. Credille, M. Kalaj, J. B. DeCoste, G. W. Peterson, T. M. Tovar, S. M. Cohen, *Chem. Commun.* **2018**, *54*, 5768-5771.

[11] a) S. H. Jungbauer, S. M. Huber, *J. Am. Chem. Soc.* **2015**, *137*, 12110-12120; b) J.-P. Gliese, S. H. Jungbauer, S. M. Huber, *Chem. Commun.* **2017**, *53*, 12052-12055.

[12] D. Cinčić, T. Friščić, *Cryst. Eng. Comm.* **2014**, *16*, 10169-10172.

[13] G. C. Shearer, S. Chavan, J. Ethiraj, J. G. Vitillo, S. Svelle, U. Olsbye, C. Lamberti, S. Bordiga, K. P. Lillerud, *Chem. Mater.* **2014**, *26*, 4068-4071.

[14] a) G. Cavallo, P. Metrangolo, R. Milani, T. Pilati, A. Priimagi, G. Resnati, G. Terraneo, *Chem. Rev.* **2016**, *116*, 2478-2601; b) P. Politzer, J. S. Murray, T. Clark, *Phys. Chem. Chem. Phys.* **2013**, *15*, 11178-11189.

[15] a) K. P. Carter, M. Kalaj, A. Kerridge, C. L. Cahill, *Cryst. Eng. Comm.* **2018**, *20*, 4916-4925; b) K. P. Carter, M. Kalaj, R. G. Surbella, III, L. C. Ducati, J. Autschbach, C. L. Cahill, *Chem. Eur. J.* **2017**, *23*, 15355-15369; c) K. P. Carter, R. G. Surbella, III, M. Kalaj, C. L. Cahill, *Chem. Eur. J.* **2018**, *24*, 12747-12756; d) M. Kalaj, K. P. Carter, C. L. Cahill, *Eur. J. Inorg. Chem.* **2017**, *2017*, 4702-4713.

[16] Y. Zhao, D. G. Truhlar, *J. Chem. Phys.* **2006**, *125*, 194101.

[17] D. Troya, *J. Phys. Chem. C* **2016**, *120*, 29312-29323.